Biointerface Research in Applied Chemistry
Open-Access Journal (ISSN: 2069-5837)

*Article*
**Volume 16, Issue 4, 2026, 118**
https://doi.org/10.33263/BRIAC164.118

# Bioactive Compounds of Sungkai (*Peronema canescens* Jack) as Natural Antiallergen: In Silico Study

**Muhammad Marsha Azzami Hasibuan [1,*], Farel Immanuel W. Purba [1], Laila Rahmah Maulidyani [1], Syahida Zulfa Raihani [1]**

[1] Department of Biochemistry, IPB University, Bogor, 16680, Indonesia; farelpurba09@gmail.com (F.I.W.P.); lailarhmhmaulidyani@gmail.com (L.R.M.); syahidazull04@gmail.com (S.Z.R.);
* Correspondence: m.marsha2001@gmail.com;

**Received: 23.05.2025; Accepted: 20.07.2025; Published: 15.08.2026**

**Abstract:** Allergies represent a significant global health concern, manifesting when allergens cross-link immunoglobulin E (IgE) bound to high-affinity FcεRI receptors on mast cells, triggering the release of the inflammatory mediators responsible for allergic symptoms. Synthetic antihistamines have been shown to be effective in reducing allergy symptoms, but they are associated with potent side effects. Natural antihistamines derived from plant secondary metabolites have attracted attention for their potential efficacy and fewer side effects. Sungkai (*Peronema canescens*) leaves contain bioactive compounds that can act as natural antihistamines. The study is supplemented by consideration of reports on additional properties with potential application in structure-activity relationships (SAR) research for the development of therapeutic drugs, as well as bioactivity radars related to the drug-like behavior of the studied compounds. Based on the results of Lipinski's rule of 5 and ADMET pharmacokinetic screening, followed by molecular screening of the histamine 1 receptor, two compounds with potential antihistamine activity were obtained. The compounds were DTXSID80244086 and Genkwanin. DTXSID80244086 has a strong binding energy of 8.36 kcal/mol but does not interact with key sites on the H1 Receptor. The second compound, Genkwanin, has more potential as an antihistamine due to its binding energy, which is competitive with Loratadine (8.35 vs 6.31 kcal/mol) but lower than Doxepin (8.35 vs 11.53 kcal/mol). DFT results showed that both DTXSID80244086 and Genkwanin have potential as drug-like molecules. Based on these results, it can be concluded that genkwanin can serve as an alternative histamine H1 receptor inhibitor, replacing Doxepin and Loratadine, the latest generation of antihistamine drugs.

**Keywords:** antihistamine inhibitor; molecular docking; Sungkai; YASARA.

© 2026 by the authors. This article is an open-access article distributed under the terms and conditions of the Creative Commons Attribution (CC BY) license (https://creativecommons.org/licenses/by/4.0/), which permits unrestricted use, distribution, and reproduction in any medium, provided the original work is properly cited. The authors retain copyright of their work, and no permission is required from the authors or the publisher to reuse or distribute this article, as long as proper attribution is given to the original source.

## 1. Introduction

Allergies represent a significant global health concern, manifesting when allergens bind immunoglobulin E (IgE) on high-affinity FcεRI receptors on mast cells, triggering the release of inflammatory mediators responsible for allergic symptoms [1]. IgE antibody-mediated allergic reactions consist of three phases: sensitization, activation, and effector. In the sensitization phase, allergens enter the body through the mucosal surfaces. Antigen-presenting cells (APCs) capture and process allergens into peptide fragments, which are then presented to major histocompatibility complex (MHC) class II molecules.

Surfactant protein-mediated phagocytosis of allergens differs in distribution and variation for different allergens. T helper (Th2) cells then activate B cells to differentiate into plasma cells that produce IgE antibodies. During the activation phase, IgE antibodies bind to the allergen upon re-exposure. Effector cells such as mast cells, eosinophils, and basophils recognize the IgE-allergen complex via FcεRI or FcεRII receptors, triggering immune response activation. In the effector phase, effector cells release inflammatory mediators, such as cytokines, histamine, prostaglandins, and leukotrienes, which cause inflammation, smooth muscle contraction, excessive mucus secretion, vasodilation, and tissue damage [2]. Allergic symptoms, including watery eyes, sneezing, hives, skin swelling, and muscle tissue inflammation, result from histamine binding to histamine H1 receptors. These receptors are responsible for vasodilation, bronchoconstriction, and mucosal secretion. H1 antihistamines block the pro-inflammatory actions of histamine by acting as inverse agonists to downregulate the H1 receptor.

Doxepin is a first-generation tricyclic H1-antihistamine (AH1R) primarily used to manage allergic symptoms and reactions. By blocking histamine receptors, it can effectively reduce a variety of histamine-mediated allergic responses, including inflammation, pruritus (itching), and urticaria (hives). Doxepin blocks H1 receptors (H1R) effectively but also crosses the blood-brain barrier (BBB), leading to central nervous system side effects, such as drowsiness and sedation. The advantages of Doxepin include its potent relief of allergic symptoms and antidepressant properties. However, its major drawbacks include sedation, anticholinergic effects (dry mouth and blurred vision), and potential impairment of cognitive and motor functions, limiting its use in certain populations [3].

Doxepin is a first-generation tricyclic H1-antihistamine (AH1R) primarily used to manage allergic symptoms and reactions. By blocking histamine receptors, it can effectively reduce a variety of histamine-mediated allergic responses, including inflammation, pruritus (itching), and urticaria (hives). Doxepin blocks H1 receptors (H1R) effectively but also crosses the blood-brain barrier (BBB), leading to central nervous system side effects, such as drowsiness and sedation. The advantages of Doxepin include its potent relief of allergic symptoms and antidepressant properties. However, its major drawbacks include sedation, anticholinergic effects (dry mouth and blurred vision), and potential impairment of cognitive and motor functions, limiting its use in certain populations [3].

Loratadine is a second-generation H1 antihistamine designed to minimize central nervous system penetration, thereby reducing sedation. It selectively blocks peripheral H1R receptors, providing effective relief of allergic symptoms with fewer sedative effects than first-generation agents [4]. The benefits of Loratadine include once-daily dosing, minimal sedation, and a favorable safety profile. However, some patients may still experience mild drowsiness, and Loratadine may be less effective than first-generation antihistamines for severe allergic reactions [5]. Natural antihistamines derived from plant secondary metabolites have attracted attention owing to their potential efficacy and fewer side effects. Sungkai (*Peronema canescens*) leaves contain bioactive compounds, such as flavonoids and tannins, that exhibit antihistaminic and anti-inflammatory properties [6]. These natural compounds can inhibit histamine release or block histamine receptors, thus offering an alternative to synthetic antihistamines. The use of Sungkai leaf extract as an antihistamine source is promising, especially for patients seeking complementary therapies with minimal adverse effects [7].

First-generation antihistamines, such as Doxepin, often cause sedation, anticholinergic effects, and cognitive impairment, while second-generation antihistamines, such as Loratadine,

although better tolerated, can still cause mild drowsiness and other side effects in some individuals [5,8]. Owing to these limitations, there is potential interest in alternative antihistamines derived from natural sources, such as Sungkai leaves, which may provide effective relief of allergy symptoms with a lower risk of side effects. This highlights the importance of exploring plant-based antihistamines as safe options for allergy management. This study aimed to investigate the potential bioactive compounds in Sungkai leaves (Peronema canescens) as natural antiallergens using an *in silico* approach.

## 2. Materials and Methods

### *2.1. Materials.*

This study was conducted on a computer running Windows 11 Professional 64-bit, an x64-based processor, and an AMD Ryzen 5 5600H @3.30 GHz-4.20 GHz. The software used was Yet Another Scientific Artificial Reality Application (YASARA) structure, BIOVIA Discovery Studio 2024, and ChimeraX. All test ligand materials were downloaded from PubChem (https://pubchem.ncbi.nlm.nih.gov), and receptors from the RCSB PDB (https://www.rcsb.org).

### *2.2. Methods.*

#### 2.2.1. Protein functional sites.

The structure of the 3RZE protein was obtained from the Protein Data Bank website (https://www.rcsb.org/). Research on the functional sites of the identified protein was conducted using CD-search on the Conserved Domain Database (CDD) web server (https://www.ncbi.nlm.nih.gov/Structure/cdd/wrpsb.cgi) and FTSite Server [9–11]. Allosteric site prediction was carried out using the AllositePro web server (https://mdl.shsmu.edu.cn/AST/) [12,13], and the Computed Atlas of Surface Topography of the Universe of Protein Folds (CASTpFold) was used through the web server https://cfold.bme.uic.edu/castpfold/ [14].

#### 2.2.2. Pharmacokinetic test.

Molecular structures of 53 test ligands derived from bioactive compounds of *Peronema canescens* Jack. and two comparison ligands (Doxepin and Loratadine) were obtained from PubChem. Pharmacokinetics is one of the most crucial pieces of information to gather before beginning research on the identification and creation of novel therapeutic therapies. Typically, this is accomplished using separate indicators known as absorption, distribution, metabolism, excretion, and toxicity (ADMET). Using online SwissADME software, various ADME parameters were computed for this study (swissadme.ch) [15]. pkCSM (biosig.lab.uq.edu.au/pkcsm/prediction) and Deep-PK (biosig.lab.uq.edu.au/deeppk/) were used to gain additional information related to the ADMET properties and the pharmacokinetic parameters [16,17].

#### 2.2.3. Toxicity prediction.

Toxicity of the compound was predicted to ensure these drugs were safe for human use. The analysis was performed using the ProTox-III (Tox. charite. de/protox3), a virtual lab for

the prediction of the toxicity of small molecules. The drugs were uploaded to the server, which yielded results showing the toxicity prediction in comparison to the already reported drugs, such as Gabapentin and Ibuprofen [18].

2.2.4. Ligands and receptor preparation.

The test ligands were obtained from the PubChem database. The 3RZE protein was chosen as the target receptor and imported into Yasara Structure software. The protein structure was prepared by adding a hydrogen atom, removing the water molecule, and deleting unused ligands. The test compounds were then optimized by minimizing their binding energy using the "Energy minimization" experiment in the YASARA Structure program. Both receptor and ligand were saved in a *.PDB file format [19].

2.2.5. Molecular docking between ligands and receptor.

The receptor was docked with ligands using YASARA. Redocking was performed to determine the most suitable grid-box size. This process was continued for screening purposes. The YASARA structure was used with the dock_run.mcr. The macro script was executed over 100 runs, and the Amber14 force field was used for validation. Screening uses the YASARA structure with the macrodock_runscreening.mcr set in the VINA method, runs=100, and Amber14 [19].

2.2.6. Molecular docking between ligands and receptor.

Density functional theory (DFT) calculations were performed using ORCA 6.0.1 to optimize the geometries of the selected molecular structures. Geometry optimization employed B3LYP theory and the 6-31G(d)* basis set. The highest occupied molecular orbital (HOMO) and lowest unoccupied molecular orbital (LUMO) energies were calculated using DFT. These energy values serve as the foundation for computing global chemical reactivity descriptors, including hardness (η), chemical potential (μ), softness (S), electronegativity (χ), and electrophilicity index (ω) [19,20]. All the calculations adhered to the methodology established by Talmaciu *et al.*[20], Equations 1 and 2 were used to calculate the electron affinity (A) and ionization potential (I), respectively. The chemical potential (μ), softness (S), electronegativity (χ), and electrophilicity index (ω) were calculated using equations 3 to 7, respectively.

$$I = - E_{homo} \quad (1)$$

$$A = - E_{lumo} \quad (2)$$

$$\mu = - (I + A)/2 \quad (3)$$

$$\chi = (I + A)/2 \quad (4)$$

$$\eta = (I - A)/2 \quad (5)$$

$$S = 12\mu \quad (6)$$

$$\omega = \mu 2/\eta \quad (7)$$

2.2.7. Data analysis.

BIOVIA Discovery Studio 2024 and ChimeraX version 1.8 were used to analyze and visualize the screening data in two and three dimensions. Using the YASARA structure, the (.yob) files or objects containing complexes are transformed into (.PDB) format for simpler 2D and 3D visualization with BIOVIA Discovery Studio and ChimeraX. DFT visualization was done using ChemCraft software [19].

## 3. Results and Discussion

The test ligands used in this study were 53 active compound ligands from Peronema canescens Jack and two comparison ligands, Doxepin and Loratadine. The first physicochemical test was performed using the Lipinski rules of five. 25 ligands were eliminated from the 53 ligands that were tested. ADMET parameters, including intestinal absorption, AMES toxicity, hERG blockers, carcinogenesis, and LD50, were used to test the remaining 28 ligands. All 28 ligands passed the ADMET screening and proceeded to the next phase of evaluation. Five compounds with the best Gibbs free energy values were selected by virtual screening of 28 test ligands. After docking the five ligands to the receptor, the results were compared with those for Doxepin and Loratadine. Based on the interaction between the ligand and receptor, the best ligands were visualized and compared with Doxepin and Loratadine.

### *3.1. Pharmacokinetic test.*

The Lipinski rule of five (Ro5) is a fundamental pharmacokinetic criterion used to identify drug-like compounds. It consists of criteria that measure the physicochemical properties of potential drug candidates, such as molecular weight, log P value, rotatable bonds, hydrogen bond donors and acceptors, and topological polar surface area (TPSA) [21]. Compounds that meet three or more Ro5 parameters are generally regarded as having favorable drug-like characteristics. In this study, 55 ligands were evaluated, comprising 53 test ligands derived from the bioactive compounds of Peronema canescens Jack and 2 comparative ligands, namely Doxepin and Loratadine. Among these ligands, 28 failed to fulfill Lipinski's rule. Of the 27 ligands that passed Lipinski's rule, the top five ligands were identified based on their suitability as antihistamine drug candidates (Table 1). The bioavailability radar for the top five ligands that met the bioavailability criteria, including Doxepin and Loratadine, is shown in Figure 1.

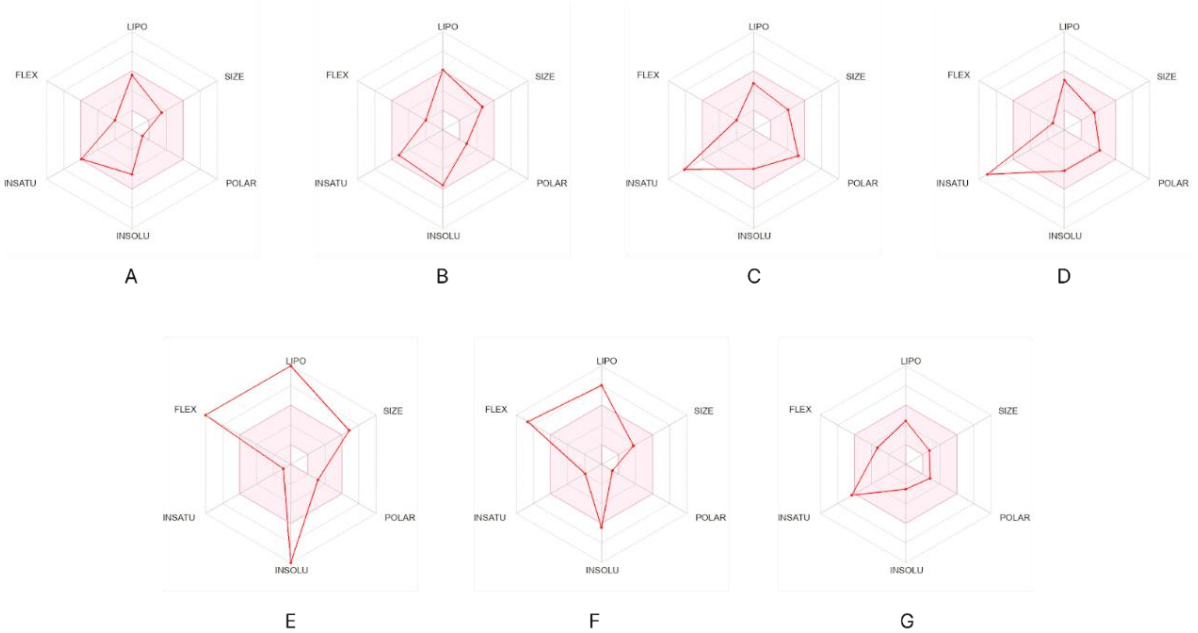


**Figure 1.** The bioavailability radars of H1R test ligands **(A)** Doxepin; **(B)** Loratadine; **(C)** DTXSID80244086; **(D)** Genkwanin; **(E)** DTXSID20887072; **(F)** DTXSID40423971; **(G)** SCHEMBL7273126.

**Table 1.** Results of Lipinski's rules of the 5 bioavailability test.

| Ligand | Lipinski's Rules of 5 | | | | | |
|---|---|---|---|---|---|---|
| | MW | Log P | RB | $H_A$ | $H_D$ | TPSA |
| Acceptable value | ≤ 500 | ≤ 5 | ≤ 10 | ≤ 10 | ≤ 5 | ≤ 140 |
| Doxepin | 279,38 | 3,96 | 3 | 2 | 0 | 12,47 |
| Loratadine | 382,89 | 4,89 | 1 | 3 | 0 | 42,43 |
| DTXSID80244086 | 330,29 | 2,59 | 3 | 7 | 3 | 109,36 |
| Genkwanin | 284,27 | 2,88 | 2 | 5 | 2 | 79,90 |
| DTXSID20887072 | 576,95 | 11,02 | 26 | 4 | 0 | 52,60 |
| DTXSID40423971 | 303,53 | 6,67 | 13 | 1 | 0 | 12,89 |
| SCHEMBL7273126 | 218,25 | 2,22 | 4 | 3 | 0 | 62,05 |

The red value indicates failure to fulfill Lipinski Ro5 test parameters.

The remaining 28 ligands were tested using ADMET parameters such as Intestinal Absorption, BBB, AMES Toxicity, hERG Blockers, Carcinogenesis, and LD50 (Table 2). All 28 ligands tested passed and advanced to the next test stage. Virtual screening identified five of the 28 tested ligands with the lowest Gibbs free energy values. The five ligands were then docked to the receptor, and the results were compared with those for Doxepin and Loratadine. Table 2 describes the result of several criteria selected from ADMET, consisting of Intestinal Absorption (>30% to be in the safe category), BBB ("Non-penetrable" result to enter the safe category), AMES Toxicity ("safe" result to enter the safe category), Human Ether-A-Go-Go Related Gene (hERG) blocker ("safe" result to enter the safe category) carcinogenesis ("Safe" result to enter the safe category), and LD50 (>300 mg/KgBW/day to enter the safe category) [16,18].

**Table 2.** Results of ADMET test.

| Ligand | ADMET | | | | | |
|---|---|---|---|---|---|---|
| | Intestinal absorption | BBB | AMES | hERG Blockers | Carcinogenesis | LD50 |
| Acceptable value | >30% | Non-Penetrable | Safe | Safe | Safe | ≥300 mg/kg |
| Doxepin | 98.19 | Penetrable | Safe | Toxic | Safe | 135 mg/kg |
| Loratadine | 95.83 | Penetrable | Safe | Toxic | Safe | 657 mg/kg |
| DTXSID80244086 | 84.84 | Penetrable | Safe | Safe | Safe | 3919 mg/kg |
| Genkwanin | 93.98 | Non-Penetrable | Safe | Safe | Safe | 3919 mg/kg |
| DTXSID20887072 | 89.56 | Penetrable | Safe | Toxic | Safe | 1363 mg/kg |
| DTXSID40423971 | 92.69 | Penetrable | Safe | Toxic | Safe | 68 mg/kg |
| SCHEMBL7273126 | 97.337 | Penetrable | Safe | Safe | Toxic | 5000 mg/kg |

The red value indicates failure to fulfill one/more of the ADMET test parameters.

A compound can be considered a drug candidate if it meets the criteria of Lipinski's Rule of Five. Lipinski's Rule of Five (RO5) was introduced by Lipinski in 1997 [22]. This rule has become a widely used guideline in the process of new drug development, both in identifying active compounds through high-throughput screening and in optimizing potential candidate compounds to increase their effectiveness without reducing specificity and selectivity [23]. Ro5 was used to evaluate the solubility of the compounds in water and fat, membrane permeability, and pharmacological effectiveness. Most orally effective drugs have small molecular sizes and moderate bioavailability.

Lipinski's rule of five (Ro5) establishes several key parameters for assessing a compound's potential as an effective oral drug candidate. The first parameter includes molecular weight, which ideally should not exceed 500 Dalton because compounds with large molecular weights tend to be difficult to absorb optimally by the body [24]. The molecular weight results for the test compounds in Table 1 show that one compound, DTXSID20887072,

has a molecular weight exceeding 500 Dalton. This means that the compound does not fulfill one of Lipinski's rules.

To measure the lipophilicity of a compound, the logP value should be below 5 and positive to ensure a balance between aqueous solubility and the ability to cross lipid membranes [25]. Compounds with high logP values tend to be more hydrophobic, which can negatively impact oral solubility and bioavailability. Compounds that are too hydrophobic may precipitate, thereby inhibiting their efficient release [25]. The results in Table 1 show that compounds DTXSID20887072 and DTXSID40423971 had LogP values above 5. Both compounds are more hydrophobic than the other ligands, making them difficult to penetrate lipid membranes.

The number of hydrogen bond donors should be no more than five, and the number of hydrogen bond acceptors should be no more than 10 [26]. All compounds in Table 1 are in the ideal state, as they do not exceed the criteria for this parameter. Hydrogen bonding plays an important role in structural stability, enzyme catalysis, and drug permeability. Functional groups capable of forming hydrogen bonds can increase the solubility and interactions of compounds with target biomolecules. However, if the number of hydrogen bond donors and acceptors is excessive, the ability of the compound to penetrate cell membranes can be reduced.

The number of rotatable bonds (RBs) plays an important role in maintaining the molecule's flexibility, enabling it to continue interacting optimally with amino acids on the active site of the enzyme. RBs are single bonds not included in the ring structure that can rotate freely and connect with heavy atoms other than hydrogen atoms at nonterminal positions [27]. Molecules that lack RBs tend to have rigid structures. This degree of flexibility also affects a compound's crystallization properties and oral bioavailability. Compounds with RB counts less than 10 exhibit better oral bioavailability, more rigid structures, and a greater tendency to crystallize [28]. Conversely, too many RBs can reduce crystallization tendency and inhibit membrane absorption. Therefore, the developed compounds with RB amounts less than 5 are considered to have strong potential for optimal oral absorption [27]. The results in Table 1 show that DTXSID20887072 and DTXSID40423971 do not meet the criteria for this parameter.

Topological Polar Surface Area (TPSA) measures the surface area of a molecule consisting of polar atoms such as oxygen, nitrogen, and hydrogen bound to them. This parameter is used to estimate the drug's ability to undergo intestinal absorption and to cross the blood-brain barrier (BBB). Molecules with TPSA values below 140 Å² generally have good intestinal absorption, whereas TPSA values below 60 Å² indicate high BBB penetration [27]. The results in Table 1 show that some compounds have good oral absorption potential and do not easily penetrate the BBB, including DTXSID80244086 (109.36 Å²), Genkwanin (79.9 Å²), and SCHEMBL7273126 (62.05 Å²). Meanwhile, the compounds Doxepin (12.47 Å²) and DTXSID40423971 (12.89 Å²) have very low TPSA values, thus potentially penetrating the BBB and causing side effects such as drowsiness [29].

Candidate therapeutic compounds were further analyzed to evaluate their absorption, distribution, metabolism, and excretion, as well as their potential toxicity in the human body. Target-based drug discovery remains the most commonly employed strategy for developing new pharmaceuticals. However, the majority of novel drug candidates fail during clinical trials owing to inadequate efficacy or safety concerns. ADMET characteristics play a critical role in determining a compound's success throughout the drug development pipeline. A variety of experimental and computational methods have been developed to economically assess ADME

properties in terms of both time and cost. These developments include both in vitro and in vivo testing. As in vitro and in vivo experimental data have accumulated, the accuracy of in silico models has significantly improved. Consequently, in silico strategies for predicting ADMET properties have become highly promising owing to their cost-effectiveness and high-throughput capabilities compared to traditional experimental methods [30].

Candidate therapeutic compounds were further analyzed to evaluate their absorption, distribution, metabolism, and excretion, as well as their potential toxicity in the human body. Target-based drug discovery remains the most commonly employed strategy for the development of new pharmaceuticals. However, the majority of novel drug candidates fail during clinical trials owing to inadequate efficacy or safety concerns. ADMET characteristics play a critical role in determining a compound's success throughout the drug development pipeline. A variety of experimental and computational methods have been developed to economically assess ADME properties in terms of both time and cost. These developments include both in vitro and in vivo testing. As in vitro and in vivo experimental data have accumulated, the accuracy of in silico models has significantly improved. Consequently, in silico strategies for predicting ADMET properties have become highly promising owing to their cost-effectiveness and high-throughput capabilities compared to traditional experimental methods [30].

The five key pharmacokinetic and toxicological parameters, absorption, distribution, metabolism, excretion, and toxicity (ADMET), summarize crucial aspects that must be thoroughly evaluated following the identification of biologically active lead compounds. Compounds that failed to meet the acceptable ADMET criteria were excluded from further development, ensuring that only candidates with favorable pharmacokinetic and toxicity profiles advanced to subsequent stages [31]. Table 2 presents the ADMET analysis data for the 55 ligand candidates. Among them, a subset of compounds passed Lipinski’s Rule of Five screening, and 28 compounds proceeded to ADMET parameter evaluation. This subset included seven candidate antihistamine ligands, two reference drugs (Doxepin and Loratadine), and five newly identified candidate compounds. Intestinal absorption, which refers to the fraction of an administered dose that reaches the systemic circulation, is a key determinant for assessing a drug’s bioavailability. High intestinal absorption signifies better bioavailability, as orally administered compounds must cross the intestinal epithelial lining, enter the systemic circulation, and interact with biological targets such as receptors, ion channels, and enzymes throughout the body [32]. All ligand candidates listed in Table 2 demonstrated intestinal absorption rates exceeding 80%, indicating excellent oral bioavailability.

The blood-brain barrier (BBB) is a selectively permeable membrane composed of endothelial cells that protects the central nervous system (CNS) from potentially harmful blood-borne substances while allowing essential nutrients and molecules to pass through [33]. BBB penetration is crucial for CNS-targeted drugs, but undesirable for non-CNS drugs to avoid central side effects. The antihistamine drug candidates in this study were designed to target the H1 receptor without affecting the BBB; thus, BBB non-permeability is a critical success factor. The experimental results in Table 2 indicate that only Genkwanin passed this test. The AMES test is a mutagenicity assay that utilizes specific bacterial strains to identify the potential of chemical compounds to induce genetic damage and cause DNA mutations [34]. As shown in Table 2, seven ligand candidates were predicted to be non-mutagenic. The evaluation of potential human Ether-à-go-go-Related Gene (hERG) potassium channel inhibition is crucial for assessing the cardiotoxicity risk of a drug, given its role in cardiac repolarization. hERG

channel inhibition can prolong the QT interval on an electrocardiogram, which in severe cases can lead to sudden cardiac death [16]. Ideally, antihistamine drug candidates should not exhibit hERG channel-blocking activity or display only very weak inhibition. According to the results in Table 2, two reference drugs (Doxepin and Loratadine) and two additional candidate ligands (DTXSID20887072 and DTXSID40423971) failed this test.

Some compounds may exert carcinogenic effects through interactions with DNA or disruption of cellular pathways, and this potential must be evaluated during drug discovery. Carcinogenicity can be predicted using chemical structure analysis, quantitative structure–activity relationship (QSAR) models, chemical categorization, read-across techniques, and physiologically based pharmacokinetic/toxicokinetic (PBPK/PBTK) modeling [35]. As shown in Table 2, SCHEMBL7273126 was identified as potentially carcinogenic and was therefore not recommended as a lead drug candidate. Various drugs can induce acute toxicity, which can manifest rapidly or over time, often depending on the dose. Acute toxicity is evaluated through chemical exposure via oral, dermal, or inhalation routes. The median lethal dose (LD50) is a primary indicator of acute toxicity, representing the dose at which 50% of the test subjects are lethally affected [36]. As shown in Table 2, SCHEMBL7273126 was identified as potentially carcinogenic and was therefore not recommended as a lead drug candidate. Various drugs can induce acute toxicity, which can manifest rapidly or over time, often depending on the dose. Acute toxicity is evaluated through chemical exposure via oral, dermal, or inhalation routes. The median lethal dose (LD50) is a primary indicator of acute toxicity, representing the dose at which 50% of the test subjects are lethally affected [36]. Toxicity was classified as extremely toxic (<5 mg/kg), highly toxic (5–50 mg/kg), moderately toxic (50–500 mg/kg), slightly toxic (500–5,000 mg/kg), practically non-toxic (5,000–15,000 mg/kg), or relatively harmless (>15,000 mg/kg) [18]. Based on the LD50 data in Table 2, the reference drug doxepin and compound DTXSID40423971 fell into the moderately toxic category (135 mg/kg and 68 mg/kg, respectively), indicating significant acute toxicity and raising concerns regarding their suitability for further development unless used in severe conditions with no safer alternatives.

### *3.2. Molecular docking between ligands and receptor.*

The grid box size used for screening was 2 Å because it yielded an RMSD of 0.68 and a binding energy of 11.53 kcal/mol during redocking. This study provides screening results in terms of binding energy, residual contact, and interaction types. The H1 Histamine (PDB: 3RZE) has a conserved functional site predicted by the conserved domain database (CDD) server, which is Asp107, Ile115, Phe424, Trp428, and Phe432 residues, whereas the non-conserved residues Trp158 and Asn198 in the pocket make only minor hydrophobic interactions with doxepin [37]. FTSite results showed that residues Ile115, Pro191, Thr194, Phe424, Trp428, Phe435, Ile454, and Tyr458 act as binding residues [11]. Table 4 lists the rankings of the top five ligands, based on their binding energies. A positive score indicates the best binding energy for the YASARA structure. Thus, a score with a more positive result indicates better binding of the ligand to the receptor. Receptor interactions with Doxepin are shown in Figure 2, receptor interactions with Loratadine are shown in Figure 3, receptor interactions with DTXSID80244086 are shown in Figure 4, and receptor interactions with Genkwanin are shown in Figure 5.

Doxepin was used as a binding energy control, so that the test ligand with a binding energy above Doxepin can be considered a potential ligand for development. Based on Table 3, the ligand used as a control (CID_667477) had a binding energy of 11.53 kcal/mol. The

binding energies of all the test ligands were lower than those of Doxepin. The highest binding energy was achieved by DTXSID80244086 (8.36 kcal/mol), followed by Genkwanin (8.35 kcal/mol), DTXSID20887072 (8.20 kcal/mol), DTXSID40423971 (8.16 kcal/mol), SCHEMBL7273126 (7.90 kcal/mol), and the lowest binding energy was Loratadine (6.31 kcal/mol), a generation 2 antihistamine drug. The YASARA structure identified the best score by sorting the best receptor–ligand complex. Therefore, a more positive score indicates better ligand-receptor binding [19].

**Table 3.** Sungkai molecular docking results with H1R receptor.

| Ligand | Effi (kcal/mol*atom) | Bind. energy (kcal/mol) | Dissoc. constant (pM) |
|---|---|---|---|
| Doxepin | 0.55 | 11.53 | 3.53E+03 |
| Loratadine | 0.23 | 6.31 | 2.37E+07 |
| DTXSID80244086 | 0.35 | 8.36 | 7.44E+05 |
| Genkwanin | 0.40 | 8.35 | 7.54E+05 |
| DTXSID20887072 | 0.20 | 8.20 | 9.61E+05 |
| DTXSID40423971 | 0.37 | 8.16 | 1.03E+06 |
| SCHEMBL7273126 | 0.55 | 7,90 | 1.61E+06 |

The red ligand violates one/more of the pharmacokinetic test parameters.

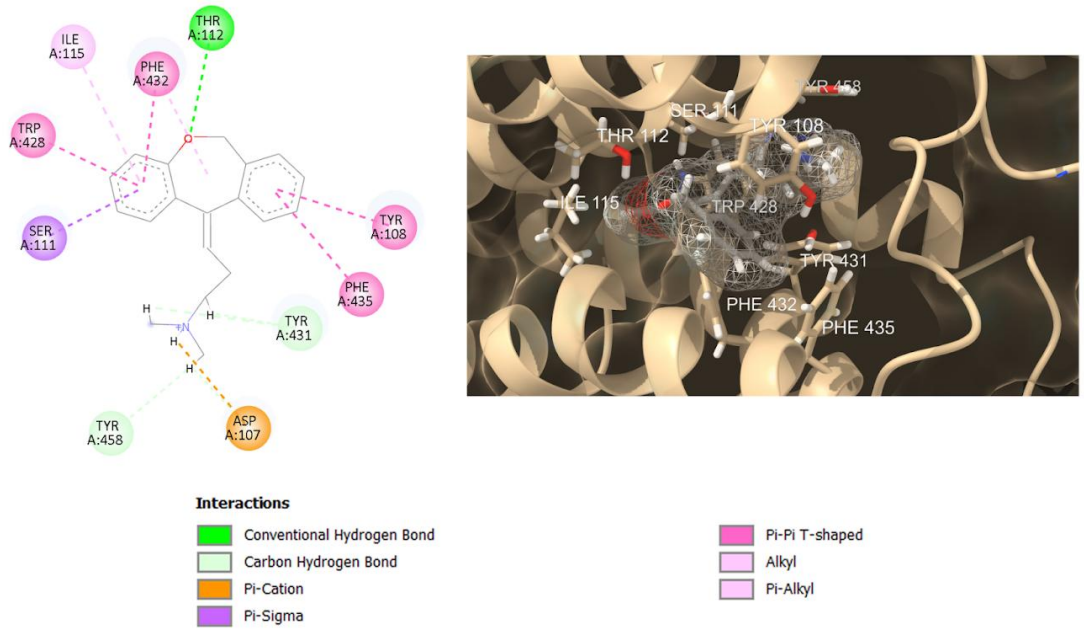


**Figure 2.** 2D visualization and 3D visualization of Doxepin interaction with H1R.

A low dissociation constant (Kd) value signifies that a ligand or binding molecule exhibits a high affinity for its receptor or target. Kd quantifies the concentration of the ligand at which half of the binding sites are occupied. Thus, a smaller Kd value indicates that fewer ligands are required to achieve half-saturation, reflecting stronger, more stable interactions [38]. The ligand efficiency of DTXSID80244086 was 0.35, whereas that of Genkwanin was 0.40, indicating that the binding energy contributed per atom of the compounds was close to the energy required to develop key contacts with the doxepin site target [19]. Based on Lipinski Ro5 and ADMET results, followed by molecular docking with the Antihistamine H1 receptor, we selected both DTXSID80244086 and Genkwanin as the best test ligands for potential alternative inhibitors.

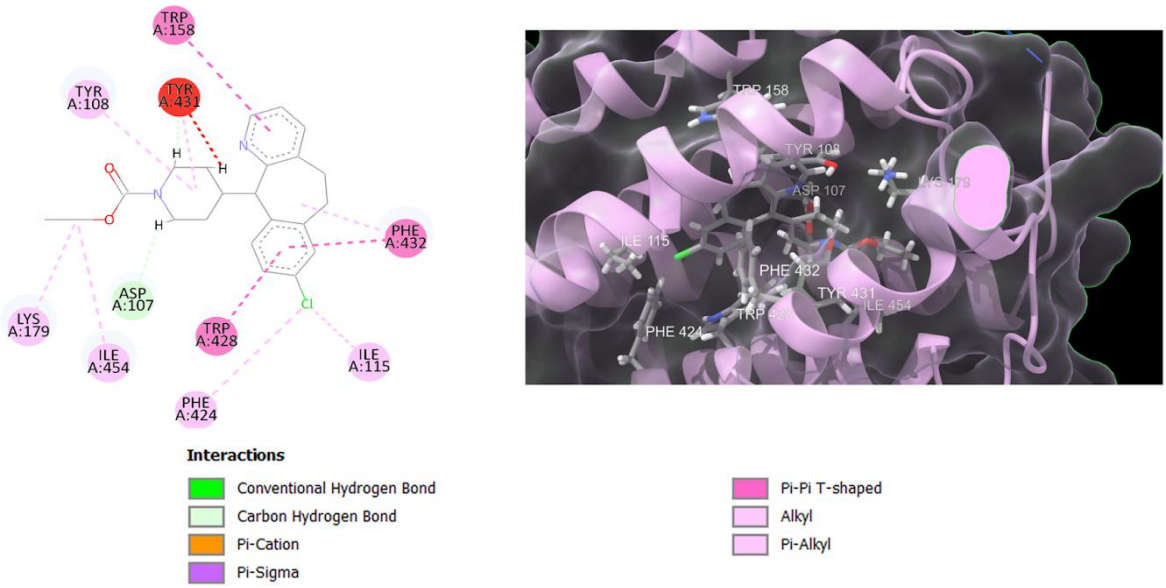


**Figure 3.** Loratadine interaction with H1R receptor visualized in 2D and 3D.

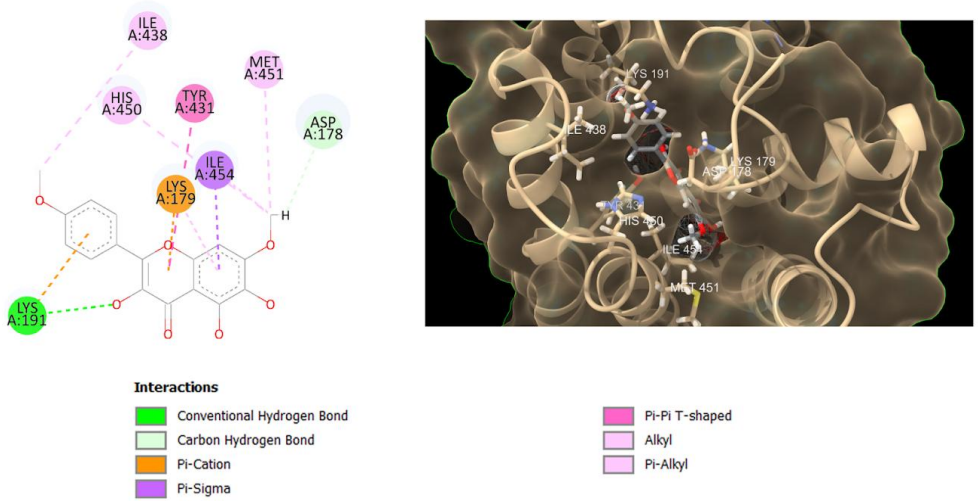


**Figure 4.** DTXSID80244086 interaction with H1R receptor visualized in 2D and 3D.

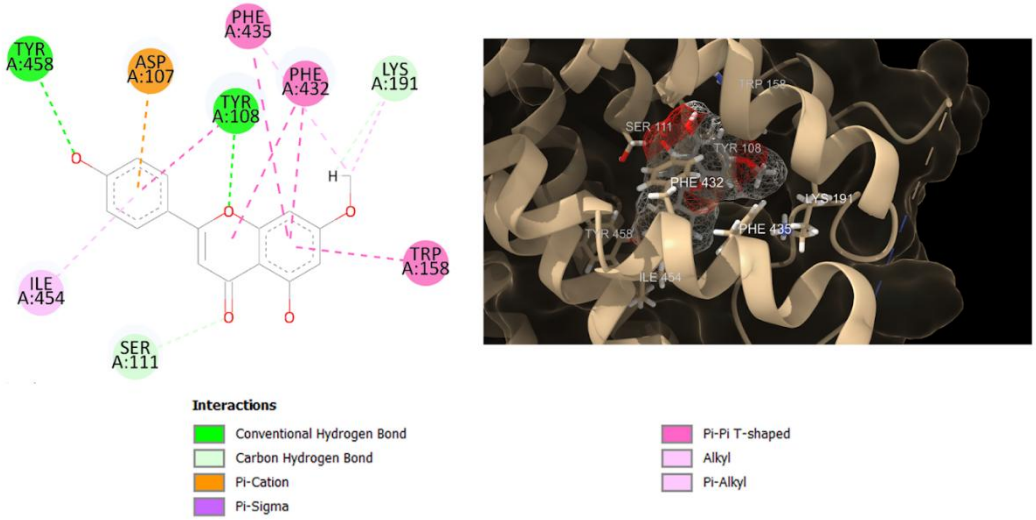


**Figure 5.** 2D visualization and 3D visualization of Genkwanin interaction with H1R.

**Table 4.** Residue interaction analysis between test ligands and H1R receptor.

| Ligand | Residues/amino acids involved | |
|---|---|---|
| | **Hydrophobic interaction** | **Hydrogen bond** |
| Doxepin | **Asp107**, Tyr431, Tyr458 | Tyr108, Ser111, **Ile115**, **Trp428**, **Phe432**, Phe435 |
| Loratadine | **Asp107**, Tyr431 | **Ile115**, Trp158, Lys179, **Phe424**, **Phe428**, Tyr431, **Phe432**, Ile454 |
| DTXSID80244086 | Lys191, Asp178, Lys179 | Lys179, Tyr431, Ile438, His450, Met451, Ile454 |
| Genkwanin | Tyr108, Ser111, Lys191, Tyr458 | Tyr108, Trp158, Lys191, **Phe432**, Phe435, Ile454 |
| DTXSID20887072 | Tyr108, Asp178, Lys191 | Tyr108, Trp158, Lys179, Phe184, Lys191, **Phe424**, **Trp428**, Tyr431, **Phe432**, Phe435, Ile438, His450, Ile454, Tyr458 |
| DTXSID40423971 | Ser111 | Tyr108, Trp158, **Trp428**, Tyr431, **Phe432**, Phe 435, Ile454 |
| SCHEMBL7273126 | - | **Ile115**, Trp158, **Trp428**, Phe432 |

Amino acids in bold indicate the presence of contact with the active site and/or binding site.

Doxepin (Figure 2) is a ligand that acts as a first-generation drug standard for this study [8]. Doxepin forms hydrogen and hydrophobic interactions. Hydrogen bonds can be categorized into conventional hydrogen bonds and carbon-hydrogen bonds. A conventional hydrogen bond is established at residue Thr112 (2.5 Å), while carbon-hydrogen bonds are formed at residues Asp107, Tyr431, and Tyr458 (2.5-3.0 Å). The hydrophobic interactions were further classified into π-sigma, π–π T-shaped, and π-alkyl bonds. The π-sigma bond is observed at residue Ser111 (2.9 Å), and the π-π shaped bond occurs at residues Tyr108, Trp428, Phe432, and Phe435 (4.81-5.7 Å). π-Alkyl bonds were identified at residues Ile115 and Phe432 (4.9-5.2 Å).

Loratadine (Figure 3) is a second-generation antihistamine that was used as a standard ligand for comparison [5]. The bonds formed are hydrogen and hydrophobic, and the hydrogen bond is a carbon-hydrogen bond between residues Asp107 and Tyr431 (2.2-2.7 A). The hydrophobic interactions were π–π T-shaped, π-alkyl, and alkyl bonds. The π-π T-shaped interaction occurs at residues Trp158, Phe428, and Phe432 (4.5-5.3 Å). Alkyl interactions occurred at residues Ile115, Lys179, and Ile454 (3.5-4.9 Å). π-Alkyl interactions occur at residues Tyr108, Phe424, Tyr431, and Phe432 (4.1-4.7 Å).

DTXSID80244086 (Figure 4) forms both hydrogen bonds and hydrophobic interactions. The hydrogen bonds identified included conventional hydrogen bonds, carbon-hydrogen bonds, and π-donor hydrogen bonds. Specifically, the conventional hydrogen bond is observed at residue Lys191 (2.6-3.0 Å), the carbon-hydrogen bond at residue Asp178 (2.8 Å), and the π-donor hydrogen bond at residue Lys179 (3.5 Å). Hydrophobic interactions occurred in π-sigma Ile454 (2,7 Å), π-π T-shaped Tyr431 (5,9 Å), Alkyl Ile437, Met451, Ile454 (3,8 - 4,9 Å), π-alkyl Lys179, and His450 (3,7 - 5,2 Å).

Genkwanin (Figure 5) emerged as the second most effective ligand based on binding energy and interactions formed, and was evaluated for its potential as an antihistamine. This compound forms both hydrogen and hydrophobic interactions. The identified hydrogen bonds included conventional hydrogen bonds and carbon-hydrogen bonds. Conventional hydrogen bonds are observed at residues Tyr108 and Tyr458 (2.7-3.0 Å), while carbon-hydrogen bonds occur at residues Ser111 and Lys191, with distances from 2.4 to 3.0 Å. Hydrophobic interactions can be categorized into three types: π-π T-shaped, alkyl, and π-alkyl bonds. π-π T-shaped interactions were observed at Tyr108, Trp158, Phe432, and Phe435, with distances between (4.7-5.7 Å). An alkyl bond was observed at Lys191, with a distance of 4.2 Å. π-Alkyl interactions occurred at residues Phe435 and Ile454, with distances ranging from 4.4 to 5.1 Å.

Table 4 lists the interactions between each test ligand, which were divided into two main categories: hydrogen bonding and hydrophobic interactions. The more hydrogen bonds a ligand has, the easier it can bind to the active site of the receptor. This specificity is essential

for accurate docking predictions and drug design, as hydrogen bonds often determine ligand selectivity for a target protein [39]. A good hydrogen bond has a distance of less than 2.3 Å. Hydrophobic interactions are considered important because of their role in stabilizing the interactions between ligands and receptors. These interactions are weaker than hydrogen bonds but can collectively have a substantial stabilizing effect by increasing entropy through the release of ordered water molecules around hydrophobic surfaces [40]. As shown in Table 4, nearly all the formed interaction bonds occurred in the active and/or binding sites, with only DTXSID80244086 not interacting with the active and/or binding residues of the H1 Histamine receptor.

Frontier molecular orbitals (FMOs) are essential for determining molecular interactions. To assess the stability and reactivity of potential drug compounds, the energy difference between the highest occupied molecular orbital (HOMO) and lowest unoccupied molecular orbital (LUMO) was determined using density functional theory (DFT) analysis. This computational approach offers significant insights into the electronic structures and properties of molecules, aiding the evaluation of their potential pharmacological activities. The energy gap between the HOMO and LUMO is a crucial indicator of a compound's chemical reactivity and stability, providing a theoretical framework for understanding its interactions with biological targets. In the scope of drug development, such molecular orbital analysis aids in the rational design and optimization of candidate compounds with desired electronic properties to improve pharmacological effectiveness [19].

Density functional theory (DFT) analysis facilitates the elucidation of electronic, vibrational, structural, and nonlinear optical properties of compounds, thereby contributing significantly to drug discovery and development. This method encompasses detailed mechanisms involving both single-drug molecules and drug delivery systems. Furthermore, DFT is often combined with molecular mechanics (MM)-based methods to investigate interactions between drugs and their receptors [41]. The parameters assessed in the present study included the highest occupied molecular orbital (HOMO), lowest unoccupied molecular orbital (LUMO), energy gap, ionization potential, electron affinity, chemical potential, electronegativity, chemical hardness, chemical softness, and electrophilicity index. The theorem explains that the energy of the highest occupied molecular orbital (E HOMO) is directly related to the ionization energy, while the energy of the lowest unoccupied molecular orbital (E LUMO) corresponds to the electron affinity. DFT calculations can determine these hardness and softness values, which can then be used to predict and understand binding affinities. These parameters work synergistically to determine the binding affinity [19].

Density functional theory calculations were performed to investigate the electrochemical properties of two standard ligands (Doxepin and Loratadine) and two chemical compounds from Peronema canescens obtained from PubChem (DTXSID80244086 and Genkwanin). The HOMO-LUMO energy gap was calculated as an indicator of molecular softness. Loratadine exhibited the most negative energy gap (-5,92 eV) (Figure 6b), followed by Genkwanin (-4.42 eV) (Figure 6d), Doxepin (-4,15 eV) (Figure 6a), and DTXSID80244086 (-3,76 eV) (Figure 6c). A lower energy gap corresponds to a softer molecule; the higher the energy gap, the greater the compound's reactivity. Moreover, the HOMO-LUMO gap represents the chemical hardness of the molecule. An increase in hardness increases the system's tendency to move towards a more stable configuration. Chemical hardness is related to the resistance of a system to deformation or polarization of its electron cloud.

Frontier molecular orbitals (FMO) were investigated to gain insight into the optical and electrical properties and potential interactions between the studied compounds (Doxepin, Loratadine, DTXSID80244086, and Genkwanin). Loratadine exhibits the greatest tendency to donate electrons, as indicated by its highest HOMO energy value of -5.92 eV, whereas Doxepin shows the weakest electron-donating capability, marked by the lowest HOMO value of -4.20 eV. Based on the LUMO values provided, the highest LUMO energy was obtained by DTXSID80244086(-1.56 eV), and the lowest was obtained by Doxepin (-0.06 eV). ΔG reflects compound stability, with a larger gap indicating greater stability. DFT results for docked ligand compounds at the H1R showed that Loratadine had a larger gap, indicating greater stability but lower reactivity. DTXSID80244086 displays the lowest energy gap of -3.76 eV, and a relatively moderate gap suggests a balance between chemical reactivity and stability. Other parameters ( η, μ, S, χ, and ω) also contribute to the binding affinity of the ligands. Based on the results shown in Table 5, DTXSID80244086 and Genkwanin are potential drug candidates with favorable DFT results.

**Table 5.** Calculation analysis of DFT studies on selected compounds.

| Compounds | Homo (eV) | Lumo (eV) | Energy gap (eV) | Ionization potential (I) (eV) | Electron affinity (A) (eV) | Chemical potentials (μ) (eV) | Electronegativity (χ) (eV) | Hardness (η) (eV) | Softness (S) (eV) | Electrophilicity index (ω) (eV) |
|---|---|---|---|---|---|---|---|---|---|---|
| Doxepin | -4.20 | -0.06 | -4.15 | 4.20 | 0.06 | -2.13 | 2.13 | 2.07 | 0.24 | 1.09 |
| Loratadine | -5.92 | -0.83 | -5.09 | 5.92 | 0.83 | -3.38 | 3.38 | 2.54 | 0.20 | 2.24 |
| DTXSID80244086 | -5.32 | -1.56 | -3.76 | 5.32 | 1.56 | -3.44 | 3.44 | 1.88 | 0.27 | 3.14 |
| Genkwanin | -5.66 | -1.24 | -4.42 | 5.66 | 1.24 | -3.45 | 3.45 | 2.21 | 0.23 | 2.70 |

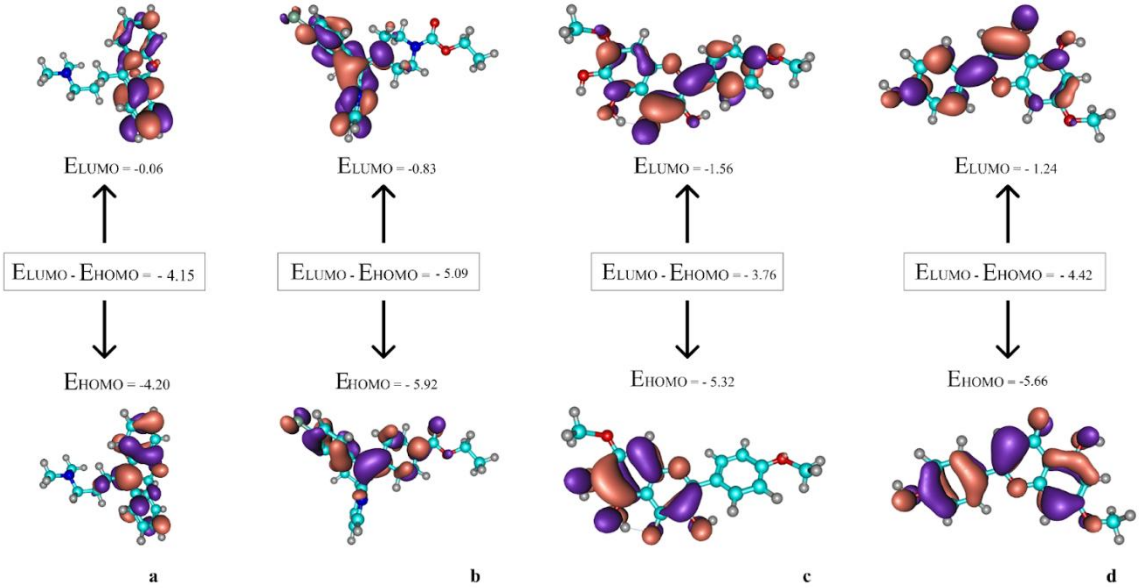


**Figure 6.** Visualization of HOMO, LUMO, and energy gap of selected compounds which were further analyzed with DFT **(a)** Doxepin; **(b)** Loratadine; **(c)** DTXSID80244086; **(d)** Genkwanin.

## 4. Conclusions

Based on the results of Lipinski's rule of 5 and ADMET pharmacokinetic screening, followed by molecular screening of the histamine 1 receptor, two compounds with potential antihistamine activity were obtained. The compounds used were DTXSID80244086 and Genkwanin. DTXSID80244086 has a strong binding energy of 8.36 kcal/mol but does not interact with key sites on the H1 Receptor. The second compound, Genkwanin, has more potential as an antihistamine due to its binding energy, which is competitive with Loratadine

(8.35 vs 6.31 kcal/mol) but lower than Doxepin (8.35 vs 11.53 kcal/mol). DFT results showed that both DTXSID80244086 and Genkwanin have potential as drug-like molecules. Based on these results, it can be concluded that genkwanin can be used as an alternative histamine H1 receptor inhibitor to replace Doxepin and Loratadine, the latest generation of antihistamine drugs. However, these results need further experimentation, both in vitro and in vivo, to bolster these findings.

## Author Contributions

Conceptualization, M.M.A.H. and F.I.W.P.; methodology, M.M.A.H., F.I.W.P., L.R.M., and S.Z.R.; software, M.M.A.H., F.I.W.P., L.R.M., and S.Z.R.; validation, M.M.A.H., F.I.W.P., L.R.M., and S.Z.R.; formal analysis, M.M.A.H., F.I.W.P., L.R.M., and S.Z.R.; investigation, M.M.A.H., F.I.W.P., L.R.M., and S.Z.R.; resources, M.M.A.H., F.I.W.P., L.R.M., and S.Z.R.; data curation, M.M.A.H., F.I.W.P., L.R.M., and S.Z.R.; writing—original draft preparation, M.M.A.H., F.I.W.P., L.R.M., and S.Z.R.; writing—review and editing, M.M.A.H., F.I.W.P., L.R.M., and S.Z.R.; visualization, M.M.A.H. and F.I.W.P.; supervision, M.M.A.H. All authors have read and agreed to the published version of the manuscript.

## Institutional Review Board Statement

Not applicable.

## Informed Consent Statement

Not applicable.

## Data Availability Statement

Data supporting the findings of this study are available upon reasonable request from the corresponding author.

## Funding

This research received no external funding.

## Acknowledgments

The author would like to thank all parties who have helped complete this research. All authors made equal contributions as the main contributors to this manuscript. No funding resource could be reported for this publication.

## Conflicts of Interest

The authors declare no conflict of interest.

## References

1. Falcon, R.M.G.; Caoili, S.E.C. Immunologic, genetic, and ecological interplay of factors involved in allergic diseases. *Front. Allergy* **2023**, *4*, 1215616, https://doi.org/10.3389/falgy.2023.1215616.
2. Thangam, E.B.; Jemima, E.A.; Singh, H.; Baig, M.S.; Khan, M.; Mathias, C.B.; Church, M.K.; Saluja, R. The role of histamine and histamine receptors in mast cell-mediated allergy and inflammation: The hunt for new therapeutic targets. *Front. Immunol.* **2018**, *9*, 1873, https://doi.org/10.3389/fimmu.2018.01873.

3. Kawauchi, H.; Yanai, K.; Wang, D.Y.; Itahashi, K.; Okubo, K. Antihistamines for allergic rhinitis treatment from the viewpoint of nonsedative properties. *Int. J. Mol. Sci.* **2019**, *20*, 213, https://doi.org/10.3390/ijms20010213.
4. Jang, J.; Hunto, S.T.; Kim, J.W.; Lee, H.P.; Kim, H.G.; Cho, J.Y. Anti-Inflammatory Activities of an Anti-Histamine Drug, Loratadine, by Suppressing TAK1 in AP-1 Pathway. *Int. J. Mol. Sci.* **2022**, *23*, 3986, https://doi.org/10.3390/ijms23073986.
5. Kong, W.; Dong, Y.; Yi, S.; Mo, W.; Yang, H. High-risks drug adverse events associated with Cetirizine and Loratadine for the treatment of allergic diseases: A retrospective pharmacovigilance study based on the FDA adverse event reporting system database. *Clin. Transl. Allergy* **2024**, *14*, e12392, https://doi.org/10.1002/clt2.12392.
6. Kokom, A.; Susilawati, Y.; Sumiwi, S.A.; Putra, O.N. Pharmacological Profile and Therapeutic Potential of Sungkai Plant (*Peronema canescens* Jack.): An Emerging Indonesian Herbal Medicine. *J. Sains Farm. Klin.* **2024**, *11*, 95–102, https://doi.org/10.25077/jsfk.11.2.95-102.2024.
7. Ahkam, A.H.; Susilawati, Y.; Sumiwi, S.A. *Peronema canescens* as a Source of Immunomodulatory Agents: A New Opportunity and Perspective. *Biology* **2024**, *13*, 744, https://doi.org/10.3390/biology13090744.
8. Myers, B.; Reddy, V.; Chan, S.; Thibodeaux, Q.; Brownstone, N.; Koo, J. Optimizing doxepin therapy in dermatology: introducing blood level monitoring and genotype testing. *J. Dermatol. Treat.* **2022**, *33*, 87–93, https://doi.org/10.1080/09546634.2020.1762841.
9. Marchler-Bauer, A.; Derbyshire, M.K.; Gonzales, N.R.; Lu, S.; Chitsaz, F.; Geer, L.Y.; Geer, R.C.; He, J.; Gwadz, M.; Hurwitz, D.I.; Lanczycki, C.J.; Lu, F.; Marchler, G.H.; Song, J.S.; Thanki, N.; Wang, Z.; Yamashita, R.A.; Zhang, D.; Zheng, C.; Bryant, S.H. CDD: NCBI's conserved domain database. *Nucleic Acids Res.* **2015**, *43*, D222–D226, https://doi.org/10.1093/nar/gku1221.
10. Marchler-Bauer, A.; Bo, Y.; Han, L.; He, J.; Lanczycki, C.J.; Lu, S.; Chitsaz, F.; Derbyshire, M.K.; Geer, R.C.; Gonzales, N.R. CDD/SPARCLE: functional classification of proteins via subfamily domain architectures. *Nucleic Acids Research* **2017**, *45*, D200-D203, https://doi.org/10.1093/nar/gkw1129.
11. Jones, G.; Jindal, A.; Ghani, U.; Kotelnikov, S.; Egbert, M.; Hashemi, N.; Vajda, S.; Padhorny, D.; Kozakov, D. Elucidation of protein function using computational docking and hotspot analysis by ClusPro and FTMap. *Acta Crystallogr. D Struct. Biol.* **2022**, *78*, 690–697, https://doi.org/10.1107/S2059798322002741.
12. Song, K.; Liu, X.; Huang, W.; Lu, S.; Shen, Q.; Zhang, L.; Zhang, J. Improved method for the identification and validation of allosteric sites. *J. Chem. Inf. Model.* **2017**, *57*, 2358–2363, https://doi.org/10.1021/acs.jcim.7b00014.
13. Huang, W.; Lu, S.; Huang, Z.; Liu, X.; Mou, L.; Luo, Y.; Zhao, Y.; Liu, Y.; Chen, Z.; Hou, T.; Zhang, J. Allosite: A method for predicting allosteric sites. *Bioinformatics* **2013**, *29*, 2357–2359, https://doi.org/10.1093/bioinformatics/btt399.
14. Ye, B.; Tian, W.; Wang, B.; Liang, J. CASTpFold: Computed Atlas of Surface Topography of the universe of protein Folds. *Nucleic Acids Res.* **2024**, *52*, W194–W199, https://doi.org/10.1093/nar/gkae415.
15. Daina, A.; Michielin, O.; Zoete, V. SwissADME: A free web tool to evaluate pharmacokinetics, drug-likeness and medicinal chemistry friendliness of small molecules. *Sci. Rep.* **2017**, *7*, 42717, https://doi.org/10.1038/srep42717.
16. Pires, D.E.V.; Blundell, T.L.; Ascher, D.B. pkCSM: Predicting small-molecule pharmacokinetic and toxicity properties using graph-based signatures. *J. Med. Chem.* **2015**, *58*, 4066–4072, https://doi.org/10.1021/acs.jmedchem.5b00104.
17. Flores-Holguín, N.; Frau, J.; Glossman-Mitnik, D. *In silico* pharmacokinetics, ADMET Study and conceptual DFT analysis of two plant cyclopeptides isolated from rosaceae as a computational peptidology approach. *Front. Chem.* **2021**, *9*, 708364, https://doi.org/10.3389/fchem.2021.708364.
18. Banerjee, P.; Kemmler, E.; Dunkel, M.; Preissner, R. ProTox 3.0: A webserver for the prediction of toxicity of chemicals. *Nucleic Acids Res.* **2024**, *52*, W513–W520, https://doi.org/10.1093/nar/gkae303.
19. Gholam, G.M.; Mahendra, F.R.; Irsal, R.A.P.; Dwicesaria, M.A.; Ariefin, M.; Kristiadi, M.; Rizki, A.F.M.; Azmi, W.A.; Artika, I.M.; Siregar, J.E. Computational exploration of compounds in *Xylocarpus granatum* as a potential inhibitor of *Plasmodium berghei* using docking, molecular dynamics, and DFT studies. *Biochem. Biophys. Res. Commun.* **2024**, *733*, 150684, https://doi.org/10.1016/j.bbrc.2024.150684.

20. Talmaciu, M.M.; Bodoki, E.; Oprean, R. Global chemical reactivity parameters for several chiral beta-blockers from the density functional theory viewpoint. *Clujul Med.* **2016**, *89*, 513–518, https://doi.org/10.15386/cjmed-610.
21. Fatiningtyas, F.A.; Napitupulu, R.; Malik, A.; Helianti, I. *In Silico* and *In Vitro* Inhibitory Activity of Indonesian Herbal Compound Extracts against SARS-COV-2 Recombinant Papain-Like Protease. *HAYATI J. Biosci.* **2025**, *32*, 356–366, https://doi.org/10.4308/hjb.32.2.356-366.
22. Nhlapho, S.; Nyathi, M.H.L.; Ngwenya, B.L.; Dube, T.; Telukdarie, A.; Munien, I.; Vermeulen, A.; Chude-Okonkwo, U.A.K. Druggability of Pharmaceutical Compounds Using Lipinski Rules with Machine Learning. *Sci. Pharm. Drug.* **2024**, *5*, 264, https://doi.org/10.58920/sciphar0304264.
23. Roskoski, R. Rule of five violations among the FDA-approved small molecule protein kinase inhibitors. *Pharmacol. Res.* **2023**, *191*, 106774, https://doi.org/10.1016/j.phrs.2023.106774.
24. Bendjedid, S.; Benouchenne, D. *In silico* studies for assessing physicochemical, pharmacokinetic and cytotoxicity properties of bioactive molecules identified by LC-MS in *Aloe vera* leaves extracts. *S. Afr. J. Bot.* **2023**, *157*, 75–81, https://doi.org/10.1016/j.sajb.2023.03.052.
25. Septiana, I.; Purwono, B.; Anwar, C.; Nurohmah, B.A.; Syahri, J. Synthesis and Docking Study of 2–Aryl-4,5-diphenyl-1H-imidazole Derivatives as Lead Compounds for Antimalarial Agent. *Indones. J. Chem.* **2022**, *22*, 105–113, https://doi.org/10.22146/ijc.67777.
26. Hajji, H.; Alaqarbeh, M.; Lakhlifi, T.; Ajana, M.A.; Alsakhen, N.; Bouachrine, M. Computational approach investigation bioactive molecules from *Saussurea Costus* plant as SARS-CoV-2 main protease inhibitors using reverse docking, molecular dynamics simulation, and pharmacokinetic ADMET parameters. *Comput. Biol. Med.* **2022**, *150*, 106209, https://doi.org/10.1016/j.compbiomed.2022.106209.
27. Ibrahim, A.; Siswandono; Prajogo, E.W.B. Cytotoxic activity of *Peronema canescens* Jack leaves on human cells: HT-29 and primary adenocarcinoma colon cancer. *Pharmacogn. J.* **2021**, *13*, 1389–1396, https://doi.org/10.5530/PJ.2021.13.176.
28. Stefaniu, A.; Pirvu, L.C. *In Silico* Study Approach on a Series of 50 Polyphenolic Compounds in Plants; A Comparison on the Bioavailability and Bioactivity Data. *Molecules* **2022**, *27*, 1413, https://doi.org/10.3390/molecules27051413.
29. Kaneko, H.; Korenaga, R.; Nakamura, R.; Kawai, S.; Ando, T.; Shiroishi, M. Binding characteristics of the doxepin E/Z-isomers to the histamine H1 receptor revealed by receptor-bound ligand analysis and molecular dynamics study. *J. Mol. Recognit.* **2024**, *37*, e3098, https://doi.org/10.1002/jmr.3098.
30. Fogel, D.B. Factors associated with clinical trials that fail and opportunities for improving the likelihood of success: A review. *Contemp. Clin. Trials Commun.* **2018**, *11*, 156–164, https://doi.org/10.1016/j.conctc.2018.08.001.
31. Saleem, U.; Bibi, S.; Shah, M.A.; Ahmad, B.; Saleem, A.; Chauhdary, Z.; Anwar, F.; Javaid, N.; Hira, S.; Akhtar, M.F.; Shah, G.M.; Khan, M.S.; Muhammad, H.; Qasim, M.; Alqarni, M.; Algarni, M.A.; Blundell, R.; Vargas-De-La-Cruz, C.; Herrera-Calderon, O.; Alhasani, R.H. Anti-Parkinson's evaluation of *Brassica juncea* leaf extract and underlying mechanism of its phytochemicals. *Front. Biosci.* **2021**, *26*, 1031–1051, https://doi.org/10.52586/5007.
32. Esaki, T.; Ohashi, R.; Watanabe, R.; Natsume-Kitatani, Y.; Kawashima, H.; Nagao, C.; Komura, H.; Mizuguchi, K. Constructing an *In Silico* Three-Class Predictor of Human Intestinal Absorption With Caco-2 Permeability and Dried-DMSO Solubility. *J. Pharm. Sci.* **2019**, *108*, 3630–3639, https://doi.org/10.1016/j.xphs.2019.07.014.
33. Wu, D.; Chen, Q.; Chen, X.; Han, F.; Chen, Z.; Wang, Y. The blood–brain barrier: structure, regulation, and drug delivery. *Signal Transduct. Target. Ther.* **2023**, *8*, 217, https://doi.org/10.1038/s41392-023-01481-w.
34. Medina-Barandica, J.; Contreras-Puentes, N.; Tarón-Dunoyer, A.; Durán-Lengua, M.; Alviz-Amador, A. *In-silico* study for the identification of potential destabilizers between the spike protein of SARS-CoV-2 and human ACE-2. *Inform. Med. Unlocked* **2023**, *40*, 101278, https://doi.org/10.1016/j.imu.2023.101278.
35. Tcheremenskaia, O.; Battistelli, C.L.; Giuliani, A.; Benigni, R.; Bossa, C. *In silico* approaches for prediction of genotoxic and carcinogenic potential of cosmetic ingredients. *Comput. Toxicol.* **2019**, *11*, 91–100, https://doi.org/10.1016/j.comtox.2019.03.005.
36. Morris-Schaffer, K.; McCoy, M.J. A Review of the LD$_{50}$ and Its Current Role in Hazard Communication. *ACS Chem. Health Saf.* **2021**, *28*, 25–33, https://doi.org/10.1021/acs.chas.0c00096.

37. Shimamura, T.; Shiroishi, M.; Weyand, S.; Tsujimoto, H.; Winter, G.; Katritch, V.; Abagyan, R.; Cherezov, V.; Liu, W.; Han, G.W.; Kobayashi, T.; Stevens, R.C.; Iwata, S. Structure of the human histamine H1 receptor complex with doxepin. *Nature* **2011**, *475*, 65–70, https://doi.org/10.1038/nature10236.
38. Liu, H.; Su, M.; Lin, H.X.; Wang, R.; Li, Y. Public Data Set of Protein-Ligand Dissociation Kinetic Constants for Quantitative Structure-Kinetics Relationship Studies. *ACS Omega* **2022**, *7*, 18985–18996, https://doi.org/10.1021/acsomega.2c02156.
39. Owoloye, A.J.; Ligali, F.C.; Enejoh, O.A.; Musa, A.Z.; Aina, O.; Idowu, E.T.; Oyebola, K.M. Molecular docking, simulation and binding free energy analysis of small molecules as Pf HT1 inhibitors. *PLoS ONE* **2022**, *17*, e0268269, https://doi.org/10.1371/journal.pone.0268269.
40. Li, J.; Ma, X.; Guo, S.; Hou, C.; Shi, L.; Zhang, H.; Zheng, B.; Liao, C.; Yang, L.; Ye, L.; He, X. A Hydrophobic-Interaction-Based Mechanism Triggers Docking between the SARS-CoV-2 Spike and Angiotensin-Converting Enzyme 2. *Glob. Chall.* **2020**, *4*, 2000067, https://doi.org/10.1002/gch2.202000067.
41. Ye, N.; Yang, Z.; Liu, Y. Applications of density functional theory in COVID-19 drug modeling. *Drug Discov. Today* **2022**, *27*, 1411–1419, https://doi.org/10.1016/j.drudis.2021.12.017.

## Publisher's Note & Disclaimer

The statements, opinions, and data presented in this publication are solely those of the individual author(s) and contributor(s) and do not necessarily reflect the views of the publisher and/or the editor(s). The publisher and/or the editor(s) disclaim any responsibility for the accuracy, completeness, or reliability of the content. Neither the publisher nor the editor(s) assume any legal liability for any errors, omissions, or consequences arising from the use of the information presented in this publication. Furthermore, the publisher and/or the editor(s) disclaim any liability for any injury, damage, or loss to persons or property that may result from the use of any ideas, methods, instructions, or products mentioned in the content. Readers are encouraged to independently verify any information before relying on it, and the publisher assumes no responsibility for any consequences arising from the use of materials contained in this publication.